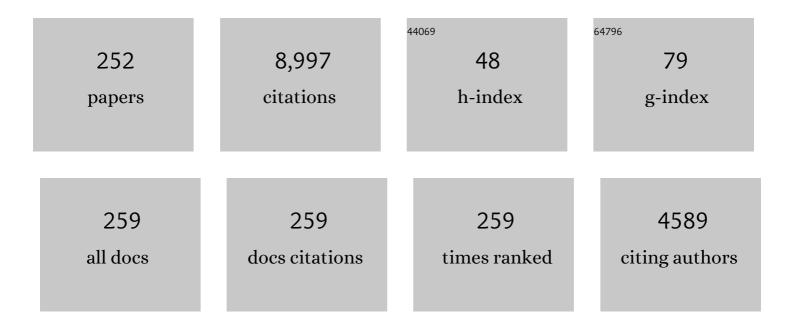
Craig J Rodger

List of Publications by Year in descending order

Source: https://exaly.com/author-pdf/5635713/publications.pdf Version: 2024-02-01



#	Article	IF	CITATIONS
1	Solar forcing for CMIP6 (v3.2). Geoscientific Model Development, 2017, 10, 2247-2302.	3.6	293
2	VLF lightning location by time of group arrival (TOGA) at multiple sites. Journal of Atmospheric and Solar-Terrestrial Physics, 2002, 64, 817-830.	1.6	287
3	Detection efficiency of the VLF World-Wide Lightning Location Network (WWLLN): initial case study. Annales Geophysicae, 2006, 24, 3197-3214.	1.6	239
4	ELF and VLF radio waves. Journal of Atmospheric and Solar-Terrestrial Physics, 2000, 62, 1689-1718.	1.6	217
5	Use of POES SEMâ $\in 2$ observations to examine radiation belt dynamics and energetic electron precipitation into the atmosphere. Journal of Geophysical Research, 2010, 115, .	3.3	209
6	Relative detection efficiency of the World Wide Lightning Location Network. Radio Science, 2012, 47, .	1.6	181
7	Impact of different energies of precipitating particles on NOx generation in the middle and upper atmosphere during geomagnetic storms. Journal of Atmospheric and Solar-Terrestrial Physics, 2009, 71, 1176-1189.	1.6	166
8	Red sprites, upward lightning, and VLF perturbations. Reviews of Geophysics, 1999, 37, 317-336.	23.0	155
9	Missing driver in the Sun–Earth connection from energetic electron precipitation impacts mesospheric ozone. Nature Communications, 2014, 5, 5197.	12.8	148
10	Diurnal variation of ozone depletion during the October-November 2003 solar proton events. Journal of Geophysical Research, 2005, 110, .	3.3	147
11	WWLL global lightning detection system: Regional validation study in Brazil. Geophysical Research Letters, 2004, 31, .	4.0	141
12	Geomagnetic activity and polar surface air temperature variability. Journal of Geophysical Research, 2009, 114, .	3.3	135
13	Energetic electron precipitation associated with pulsating aurora: EISCAT and Van Allen Probe observations. Journal of Geophysical Research: Space Physics, 2015, 120, 2754-2766.	2.4	133
14	Large solar flares and their ionosphericDregion enhancements. Journal of Geophysical Research, 2005, 110, .	3.3	131
15	Location accuracy of VLF World-Wide Lightning Location (WWLL) network: Post-algorithm upgrade. Annales Geophysicae, 2005, 23, 277-290.	1.6	128
16	Carbon emissions from international cruise ship passengers' travel to and from New Zealand. Energy Policy, 2010, 38, 2552-2560.	8.8	124
17	Far-Field Power of Lightning Strokes as Measured by the World Wide Lightning Location Network. Journal of Atmospheric and Oceanic Technology, 2012, 29, 1102-1110.	1.3	114
18	Location accuracy of long distance VLF lightning locationnetwork. Annales Geophysicae, 2004, 22, 747-758.	1.6	110

#	Article	IF	CITATIONS
19	Growing Detection Efficiency of the World Wide Lightning Location Network. , 2009, , .		106
20	Radiation belt electron precipitation due to VLF transmitters: Satellite observations. Geophysical Research Letters, 2008, 35, .	4.0	105
21	lonosphere gives size of greatest solar flare. Geophysical Research Letters, 2004, 31, n/a-n/a.	4.0	104
22	Remote sensing space weather events: Antarcticâ€Arctic Radiationâ€belt (Dynamic) Depositionâ€VLF Atmospheric Research Konsortium network. Space Weather, 2009, 7, .	3.7	102
23	Geomagnetic activity signatures in wintertime stratosphere wind, temperature, and wave response. Journal of Geophysical Research D: Atmospheres, 2013, 118, 2169-2183.	3.3	95
24	Observations of relativistic electron precipitation from the radiation belts driven by EMIC waves. Geophysical Research Letters, 2008, 35, .	4.0	93
25	POES satellite observations of EMICâ€wave driven relativistic electron precipitation during 1998–2010. Journal of Geophysical Research: Space Physics, 2013, 118, 232-243.	2.4	87
26	Total solar eclipse effects on VLF signals: Observations and modeling. Radio Science, 2001, 36, 773-788.	1.6	86
27	Contrasting the efficiency of radiation belt losses caused by ducted and nonducted whistlerâ€mode waves from groundâ€based transmitters. Journal of Geophysical Research, 2010, 115, .	3.3	79
28	Destruction of the tertiary ozone maximum during a solar proton event. Geophysical Research Letters, 2006, 33, .	4.0	75
29	Radiation belt electron precipitation into the atmosphere: Recovery from a geomagnetic storm. Journal of Geophysical Research, 2007, 112, .	3.3	75
30	First evidence of mesospheric hydroxyl response to electron precipitation from the radiation belts. Journal of Geophysical Research, 2011, 116, .	3.3	75
31	Radiation belt electron precipitation by manâ€made VLF transmissions. Journal of Geophysical Research, 2008, 113, .	3.3	73
32	Local time variation in land/ocean lightning flash density as measured by the World Wide Lightning Location Network. Journal of Geophysical Research, 2007, 112, .	3.3	71
33	Subionospheric VLF perturbations associated with lightning discharges. Journal of Atmospheric and Solar-Terrestrial Physics, 2003, 65, 591-606.	1.6	69
34	Carbon emission offsets for aviation-generated emissions due to international travel to and from New Zealand. Energy Policy, 2009, 37, 3438-3447.	8.8	66
35	Evidence of subâ€MeV EMICâ€driven electron precipitation. Geophysical Research Letters, 2017, 44, 1210-1218.	4.0	66
36	World-wide lightning location using VLF propagation in the Earth-ionosphere waveguide. IEEE Antennas and Propagation Magazine, 2008, 50, 40-60.	1.4	65

#	Article	IF	CITATIONS
37	Electron precipitation from EMIC waves: A case study from 31 May 2013. Journal of Geophysical Research: Space Physics, 2015, 120, 3618-3631.	2.4	65
38	Comparison between POES energetic electron precipitation observations and riometer absorptions: Implications for determining true precipitation fluxes. Journal of Geophysical Research: Space Physics, 2013, 118, 7810-7821.	2.4	63
39	A model providing longâ€ŧerm data sets of energetic electron precipitation during geomagnetic storms. Journal of Geophysical Research D: Atmospheres, 2016, 121, 12,520.	3.3	63
40	Sunrise effects on VLF signals propagating over a long north-south path. Radio Science, 1999, 34, 939-948.	1.6	62
41	Global Distribution of Superbolts. Journal of Geophysical Research D: Atmospheres, 2019, 124, 9996-10005.	3.3	61
42	Lower ionospheric modification by lightning-EMP: Simulation of the night ionosphere over the United States. Geophysical Research Letters, 2001, 28, 199-202.	4.0	60
43	Groundâ€based transmitter signals observed from space: Ducted or nonducted?. Journal of Geophysical Research, 2008, 113, .	3.3	60
44	Highâ€resolution in situ observations of electron precipitationâ€causing EMIC waves. Geophysical Research Letters, 2015, 42, 9633-9641.	4.0	59
45	Relaxation of transient ionization in the lower ionosphere. Journal of Geophysical Research, 1998, 103, 6969-6975.	3.3	56
46	Investigating seismoionospheric effects on a long subionospheric path. Journal of Geophysical Research, 1999, 104, 28171-28179.	3.3	54
47	Precipitating radiation belt electrons and enhancements of mesospheric hydroxyl during 2004–2009. Journal of Geophysical Research, 2012, 117, .	3.3	54
48	Significance of lightning-generated whistlers to inner radiation belt electron lifetimes. Journal of Geophysical Research, 2003, 108, .	3.3	53
49	Contrasting the responses of three different groundâ€based instruments to energetic electron precipitation. Radio Science, 2012, 47, .	1.6	53
50	Substormâ€induced energetic electron precipitation: Impact on atmospheric chemistry. Geophysical Research Letters, 2015, 42, 8172-8176.	4.0	51
51	Groundâ€based estimates of outer radiation belt energetic electron precipitation fluxes into the atmosphere. Journal of Geophysical Research, 2010, 115, .	3.3	50
52	The plasmasphere during a space weather event: first results from the PLASMON project. Journal of Space Weather and Space Climate, 2013, 3, A23.	3.3	50
53	Longâ€Lasting Geomagnetically Induced Currents and Harmonic Distortion Observed in New Zealand During the 7–8 September 2017 Disturbed Period. Space Weather, 2018, 16, 704-717.	3.7	48
54	The effects of hardâ€spectra solar proton events on the middle atmosphere. Journal of Geophysical Research, 2008, 113, .	3.3	47

#	Article	IF	CITATIONS
55	Lightning in the Arctic. Geophysical Research Letters, 2021, 48, e2020GL091366.	4.0	47
56	NO _x enhancements in the middle atmosphere during 2003–2004 polar winter: Relative significance of solar proton events and the aurora as a source. Journal of Geophysical Research, 2007, 112, .	3.3	45
57	Daytime midlatitude <i>D</i> region parameters at solar minimum from short-path VLF phase and amplitude. Journal of Geophysical Research, 2011, 116, .	3.3	45
58	Longâ€Term Geomagnetically Induced Current Observations From New Zealand: Peak Current Estimates for Extreme Geomagnetic Storms. Space Weather, 2017, 15, 1447-1460.	3.7	44
59	Dynamic geomagnetic rigidity cutoff variations during a solar proton event. Journal of Geophysical Research, 2006, 111, .	3.3	43
60	Confirmation of EMIC waveâ€driven relativistic electron precipitation. Journal of Geophysical Research: Space Physics, 2016, 121, 5366-5383.	2.4	43
61	Longâ€ŧerm geomagnetically induced current observations in New Zealand: Earth return corrections and geomagnetic field driver. Space Weather, 2017, 15, 1020-1038.	3.7	43
62	Nature's Grand Experiment: Linkage between magnetospheric convection and the radiation belts. Journal of Geophysical Research: Space Physics, 2016, 121, 171-189.	2.4	42
63	VLF line radiation observed by satellite. Journal of Geophysical Research, 1995, 100, 5681.	3.3	41
64	Modeling a large solar proton event in the southern polar atmosphere. Journal of Geophysical Research, 2005, 110, .	3.3	41
65	Determining the spectra of radiation belt electron losses: Fitting DEMETER electron flux observations for typical and storm times. Journal of Geophysical Research: Space Physics, 2013, 118, 7611-7623.	2.4	41
66	POES MEPED differential flux retrievals and electron channel contamination correction. Journal of Geophysical Research: Space Physics, 2015, 120, 4596-4612.	2.4	41
67	Pitch Angle Scattering of Subâ€MeV Relativistic Electrons by Electromagnetic Ion Cyclotron Waves. Journal of Geophysical Research: Space Physics, 2019, 124, 5610-5626.	2.4	41
68	Seeking spriteâ€induced signatures in remotely sensed middle atmosphere NO ₂ . Geophysical Research Letters, 2008, 35, .	4.0	40
69	Longitudinal hotspots in the mesospheric OH variations due to energetic electron precipitation. Atmospheric Chemistry and Physics, 2014, 14, 1095-1105.	4.9	40
70	Ionospheric evidence of thermosphere-to-stratosphere descent of polar NOX. Geophysical Research Letters, 2006, 33, .	4.0	39
71	Energetic electron precipitation during substorm injection events: Highâ€latitude fluxes and an unexpected midlatitude signature. Journal of Geophysical Research, 2008, 113, .	3.3	39
72	Direct observations of nitric oxide produced by energetic electron precipitation into the Antarctic middle atmosphere. Geophysical Research Letters, 2011, 38, n/a-n/a.	4.0	38

#	Article	IF	CITATIONS
73	Polar Ozone Response to Energetic Particle Precipitation Over Decadal Time Scales: The Role of Mediumâ€Energy Electrons. Journal of Geophysical Research D: Atmospheres, 2018, 123, 607-622.	3.3	38
74	Occurrence characteristics of relativistic electron microbursts from SAMPEX observations. Journal of Geophysical Research: Space Physics, 2017, 122, 8096-8107.	2.4	37
75	An Updated Model Providing Longâ€Term Data Sets of Energetic Electron Precipitation, Including Zonal Dependence. Journal of Geophysical Research D: Atmospheres, 2018, 123, 9891-9915.	3.3	37
76	Sprite observations in the Northern Territory of Australia. Journal of Geophysical Research, 2000, 105, 4689-4697.	3.3	36
77	The Role of Localized Compressional Ultraâ€low Frequency Waves in Energetic Electron Precipitation. Journal of Geophysical Research: Space Physics, 2018, 123, 1900-1914.	2.4	36
78	The structure of red sprites determined by VLF scattering. IEEE Antennas and Propagation Magazine, 1996, 38, 7-15.	1.4	35
79	The importance of atmospheric precipitation in storm-time relativistic electron flux drop outs. Geophysical Research Letters, 2006, 33, n/a-n/a.	4.0	35
80	Modeling Geoelectric Fields and Geomagnetically Induced Currents Around New Zealand to Explore GIC in the South Island's Electrical Transmission Network. Space Weather, 2017, 15, 1396-1412.	3.7	35
81	Substormâ€induced energetic electron precipitation: Morphology and prediction. Journal of Geophysical Research: Space Physics, 2015, 120, 2993-3008.	2.4	34
82	Transformer‣evel Modeling of Geomagnetically Induced Currents in New Zealand's South Island. Space Weather, 2018, 16, 718-735.	3.7	34
83	Temporal evolution of very strong Trimpis observed at Darwin, Australia. Geophysical Research Letters, 1997, 24, 2419-2422.	4.0	33
84	Energetic particle precipitation into the middle atmosphere triggered by a coronal mass ejection. Journal of Geophysical Research, 2007, 112, .	3.3	33
85	Determining the size of lightning-induced electron precipitation patches. Journal of Geophysical Research, 2002, 107, SIA 10-1-SIA 10-11.	3.3	32
86	Modeling polar ionospheric effects during the October-November 2003 solar proton events. Radio Science, 2006, 41, n/a-n/a.	1.6	32
87	Significance of transient luminous events to neutral chemistry: Experimental measurements. Geophysical Research Letters, 2008, 35, .	4.0	31
88	Radiation belt electron precipitation due to geomagnetic storms: Significance to middle atmosphere ozone chemistry. Journal of Geophysical Research, 2010, 115, .	3.3	31
89	Investigating energetic electron precipitation through combining groundâ€based and balloon observations. Journal of Geophysical Research: Space Physics, 2017, 122, 534-546.	2.4	31
90	A search for ELF/VLF activity associated with earthquakes using ISIS satellite data. Journal of Geophysical Research, 1996, 101, 13369-13378.	3.3	30

#	Article	IF	CITATIONS
91	Is magnetospheric line radiation man-made?. Journal of Geophysical Research, 2000, 105, 15981-15990.	3.3	30
92	Multiâ€instrument Observation of Nonlinear EMICâ€Driven Electron Precipitation at sub–MeV Energies. Geophysical Research Letters, 2019, 46, 7248-7257.	4.0	30
93	Additional stratospheric NO _{<i>x</i>} production by relativistic electron precipitation during the 2004 spring NO _{<i>x</i>} descent event. Journal of Geophysical Research, 2009, 114, .	3.3	29
94	Relationship between median intensities of electromagnetic emissions in the VLF range and lightning activity. Journal of Geophysical Research, 2010, 115, .	3.3	29
95	Longâ€ŧerm determination of energetic electron precipitation into the atmosphere from AARDDVARK subionospheric VLF observations. Journal of Geophysical Research: Space Physics, 2015, 120, 2194-2211.	2.4	29
96	Measurements of the VLF scattering pattern of the structured plasma of red sprites. IEEE Antennas and Propagation Magazine, 1998, 40, 29-38.	1.4	28
97	Modeling of subionospheric VLF signal perturbations associated with earthquakes. Radio Science, 1999, 34, 1177-1185.	1.6	28
98	Energetic particle injection, acceleration, and loss during the geomagnetic disturbances which upset Galaxy 15. Journal of Geophysical Research, 2012, 117, .	3.3	28
99	A reexamination of latitudinal limits of substormâ€produced energetic electron precipitation. Journal of Geophysical Research: Space Physics, 2013, 118, 6694-6705.	2.4	28
100	Latitudinal extent of the January 2005 solar proton event in the Northern Hemisphere from satellite observations of hydroxyl. Annales Geophysicae, 2007, 25, 2203-2215.	1.6	27
101	Relativistic microburst storm characteristics: Combined satellite and groundâ€based observations. Journal of Geophysical Research, 2010, 115, .	3.3	27
102	Temporal variability of the descent of highâ€altitude NO _X inferred from ionospheric data. Journal of Geophysical Research, 2007, 112, .	3.3	26
103	Subionospheric early VLF perturbations observed at Suva: VLF detection of red sprites in the day?. Journal of Geophysical Research, 2008, 113, .	3.3	26
104	Do Statistical Models Capture the Dynamics of the Magnetopause During Sudden Magnetospheric Compressions?. Journal of Geophysical Research: Space Physics, 2020, 125, e2019JA027289.	2.4	26
105	Atmospheric impact of the Carrington event solar protons. Journal of Geophysical Research, 2008, 113,	3.3	25
106	Carbon dioxide emissions from international air freight. Atmospheric Environment, 2011, 45, 7036-7045.	4.1	25
107	Lightning-driven inner radiation belt energy deposition into the atmosphere: implications for ionisation-levels and neutral chemistry. Annales Geophysicae, 2007, 25, 1745-1757.	1.6	25
108	Temporal properties of magnetospheric line radiation. Journal of Geophysical Research, 2000, 105, 329-336.	3.3	24

#	Article	IF	CITATIONS
109	Lowâ€latitude ionospheric <i>D</i> region dependence on solar zenith angle. Journal of Geophysical Research: Space Physics, 2014, 119, 6865-6875.	2.4	24
110	Assessment of GIC Based On Transfer Function Analysis. Space Weather, 2017, 15, 1615-1627.	3.7	24
111	Atmospheric Effects of >30â€keV Energetic Electron Precipitation in the Southern Hemisphere Winter During 2003. Journal of Geophysical Research: Space Physics, 2019, 124, 8138-8153.	2.4	24
112	Decay of a vertical plasma column: A model to explain VLF sprites. Geophysical Research Letters, 1997, 24, 2765-2768.	4.0	23
113	New Directions for Radiation Belt Research. Space Weather, 2009, 7, n/a-n/a.	3.7	23
114	Empirical determination of solar proton access to the atmosphere: Impact on polar flight paths. Space Weather, 2013, 11, 420-433.	3.7	23
115	Relativistic Electron Microburst Events: Modeling the Atmospheric Impact. Geophysical Research Letters, 2018, 45, 1141-1147.	4.0	23
116	Storm time, shortâ€lived bursts of relativistic electron precipitation detected by subionospheric radio wave propagation. Journal of Geophysical Research, 2007, 112, .	3.3	22
117	Source region for whistlers detected at Rothera, Antarctica. Journal of Geophysical Research, 2011, 116, .	3.3	22
118	Observations and Modeling of Increased Nitric Oxide in the Antarctic Polar Middle Atmosphere Associated With Geomagnetic Stormâ€Driven Energetic Electron Precipitation. Journal of Geophysical Research: Space Physics, 2018, 123, 6009-6025.	2.4	22
119	Logarithmic decay and Doppler shift of plasma associated with sprites. Journal of Atmospheric and Solar-Terrestrial Physics, 1998, 60, 741-753.	1.6	21
120	Minimum sprite plasma density as determined by VLF scattering. IEEE Antennas and Propagation Magazine, 2001, 43, 12-24.	1.4	21
121	Seeking sprite-induced signatures in remotely sensed middle atmosphere NO ₂ : latitude and time variations. Plasma Sources Science and Technology, 2009, 18, 034014.	3.1	21
122	Rapid Radiation Belt Losses Occurring During High-Speed Solar Wind Stream-Driven Storms: Importance of Energetic Electron Precipitation. Geophysical Monograph Series, 2013, , 213-224.	0.1	21
123	Comparison of modeled and observed effects of radiation belt electron precipitation on mesospheric hydroxyl and ozone. Journal of Geophysical Research D: Atmospheres, 2013, 118, 11,419.	3.3	21
124	Nonlinear and Synergistic Effects of ULF Pc5, VLF Chorus, and EMIC Waves on Relativistic Electron Flux at Geosynchronous Orbit. Journal of Geophysical Research: Space Physics, 2018, 123, 4755-4766.	2.4	21
125	Magnetospheric line radiation observations at Halley, Antarctica. Journal of Geophysical Research, 1999, 104, 17441-17447.	3.3	20
126	The atmospheric implications of radiation belt remediation. Annales Geophysicae, 2006, 24, 2025-2041.	1.6	20

#	Article	IF	CITATIONS
127	Energetic electron precipitation and auroral morphology at the substorm recovery phase. Journal of Geophysical Research: Space Physics, 2017, 122, 6508-6527.	2.4	20
128	A Distributed Lag Autoregressive Model of Geostationary Relativistic Electron Fluxes: Comparing the Influences of Waves, Seed and Source Electrons, and Solar Wind Inputs. Journal of Geophysical Research: Space Physics, 2018, 123, 3646-3671.	2.4	20
129	Characteristics of Relativistic Microburst Intensity From SAMPEX Observations. Journal of Geophysical Research: Space Physics, 2019, 124, 5627-5640.	2.4	20
130	Geomagnetically Induced Current Model Validation From New Zealand's South Island. Space Weather, 2020, 18, e2020SW002494.	3.7	20
131	Scattering of VLF from an experimentally described sprite. Journal of Atmospheric and Solar-Terrestrial Physics, 1998, 60, 765-769.	1.6	19
132	VLF scattering from red sprites: Vertical columns of ionization in the Earth-ionosphere waveguide. Radio Science, 1999, 34, 913-921.	1.6	19
133	Midlatitude ionospheric <i>D</i> region: Height, sharpness, and solar zenith angle. Journal of Geophysical Research: Space Physics, 2017, 122, 8933-8946.	2.4	19
134	Telluric Field Variations as Drivers of Variations in Cathodic Protection Potential on a Natural Gas Pipeline in New Zealand. Space Weather, 2018, 16, 1396-1409.	3.7	19
135	Geomagnetically Induced Currents and Harmonic Distortion: Stormâ€Time Observations From New Zealand. Space Weather, 2020, 18, e2019SW002387.	3.7	19
136	Modeling the relaxation of red sprite plasma. Geophysical Research Letters, 1999, 26, 3293-3296.	4.0	18
137	VLF scattering from red sprites: Application of numerical modeling. Radio Science, 1999, 34, 923-932.	1.6	18
138	REMOTE SENSING OF THE UPPER ATMOSPHERE BY VLF. , 2006, , 167-190.		18
139	Survey of magnetospheric line radiation events observed by the DEMETER spacecraft. Journal of Geophysical Research, 2009, 114, .	3.3	18
140	Links between mesopause temperatures and groundâ€based VLF narrowband radio signals. Journal of Geophysical Research D: Atmospheres, 2013, 118, 4244-4255.	3.3	18
141	Electromagnetic scattering from a group of thin conducting cylinders. Radio Science, 1997, 32, 907-912.	1.6	17
142	VLF scattering from Red Sprites—Theory. Journal of Atmospheric and Solar-Terrestrial Physics, 1998, 60, 755-763.	1.6	17
143	Are whistler ducts created by thunderstorm electrostatic fields?. Journal of Geophysical Research, 1998, 103, 2163-2169.	3.3	17
144	Validation of single-station lightning location technique. Radio Science, 2002, 37, 12-1-12-9.	1.6	17

9

#	Article	IF	CITATIONS
145	Inner radiation belt electron lifetimes due to whistler-induced electron precipitation (WEP) driven losses. Geophysical Research Letters, 2002, 29, 30-1-30-4.	4.0	17
146	Radiation belt electron precipitation fluxes associated with lightning. Journal of Geophysical Research, 2004, 109, .	3.3	17
147	The effects and correction of the geometric factor for the POES/MEPED electron flux instrument using a multisatellite comparison. Journal of Geophysical Research: Space Physics, 2014, 119, 6386-6404.	2.4	17
148	Generation of EMIC Waves and Effects on Particle Precipitation During a Solar Wind Pressure Intensification With <i>B</i> _{<i>z</i>} >0. Journal of Geophysical Research: Space Physics, 2019, 124, 4492-4508.	2.4	17
149	Comparing Electron Precipitation Fluxes Calculated From Pitch Angle Diffusion Coefficients to LEO Satellite Observations. Journal of Geophysical Research: Space Physics, 2021, 126, e2020JA028410.	2.4	17
150	Decay of whistler-induced electron precipitation and cloud-ionosphere electrical discharge Trimpis: Observations and analysis. Radio Science, 2001, 36, 151-169.	1.6	16
151	Reconsidering the effectiveness of quasi-static thunderstorm electric fields for whistler duct formation. Journal of Geophysical Research, 2002, 107, SIA 16-1.	3.3	16
152	Testing the importance of precipitation loss mechanisms in the inner radiation belt. Geophysical Research Letters, 2004, 31, n/a-n/a.	4.0	16
153	Sunset transition of negative charge in the D-region ionosphere during high-ionization conditions. Annales Geophysicae, 2006, 24, 187-202.	1.6	16
154	Automatic Whistler Detector and Analyzer system: Implementation of the analyzer algorithm. Journal of Geophysical Research, 2010, 115, .	3.3	16
155	Characteristics of precipitating energetic electron fluxes relative to the plasmapause during geomagnetic storms. Journal of Geophysical Research: Space Physics, 2014, 119, 8784-8800.	2.4	16
156	HEPPA III Intercomparison Experiment on Electron Precipitation Impacts: 1. Estimated Ionization Rates During a Geomagnetic Active Period in April 2010. Journal of Geophysical Research: Space Physics, 2022, 127, .	2.4	16
157	Space shuttle observation of an unusual transient atmospheric emission. Geophysical Research Letters, 2005, 32, .	4.0	15
158	Global lightning distribution and whistlers observed at Dunedin, New Zealand. Annales Geophysicae, 2010, 28, 499-513.	1.6	15
159	Energetic outer radiation belt electron precipitation during recurrent solar activity. Journal of Geophysical Research, 2010, 115, .	3.3	15
160	Daytime <i>D</i> region parameters from long-path VLF phase and amplitude. Journal of Geophysical Research, 2011, 116, n/a-n/a.	3.3	15
161	Comparison of Relativistic Microburst Activity Seen by SAMPEX With Groundâ€Based Wave Measurements at Halley, Antarctica. Journal of Geophysical Research: Space Physics, 2018, 123, 1279-1294.	2.4	15
162	Correlation between global lightning and whistlers observed at Tihany, Hungary. Journal of Geophysical Research, 2009, 114, .	3.3	14

#	Article	IF	CITATIONS
163	Lightning driven inner radiation belt energy deposition into the atmosphere: regional and global estimates. Annales Geophysicae, 2005, 23, 3419-3430.	1.6	13
164	Hiss from the chorus. Nature, 2008, 452, 41-42.	27.8	13
165	Temporalâ€spatial modeling of electron density enhancement due to successive lightning strokes. Journal of Geophysical Research, 2010, 115, .	3.3	13
166	Combined THEMIS and groundâ€based observations of a pair of substormâ€associated electron precipitation events. Journal of Geophysical Research, 2012, 117, .	3.3	13
167	A case study of electron precipitation fluxes due to plasmaspheric hiss. Journal of Geophysical Research: Space Physics, 2015, 120, 6736-6748.	2.4	13
168	Northern Hemisphere Stratospheric Ozone Depletion Caused by Solar Proton Events: The Role of the Polar Vortex. Geophysical Research Letters, 2018, 45, 2115-2124.	4.0	13
169	Geomagnetically Induced Currents and Harmonic Distortion: High Time Resolution Case Studies. Space Weather, 2020, 18, e2020SW002594.	3.7	13
170	The Combined Influence of Lower Band Chorus and ULF Waves on Radiation Belt Electron Fluxes at Individual <i>L</i> â€5hells. Journal of Geophysical Research: Space Physics, 2021, 126, e2020JA028755.	2.4	13
171	A quantitative estimate of the ducted whistler power within the outer plasmasphere. Journal of Atmospheric and Solar-Terrestrial Physics, 2001, 63, 61-74.	1.6	12
172	Improved dynamic geomagnetic rigidity cutoff modeling: Testing predictive accuracy. Journal of Geophysical Research, 2007, 112, .	3.3	12
173	Automatic whistler detection: Operational results from New Zealand. Radio Science, 2009, 44, .	1.6	12
174	Simultaneous observation of chorus and hiss near the plasmapause. Journal of Geophysical Research, 2012, 117, .	3.3	12
175	Mesospheric Nitric Acid Enhancements During Energetic Electron Precipitation Events Simulated by WACCMâ€D. Journal of Geophysical Research D: Atmospheres, 2018, 123, 6984-6998.	3.3	12
176	Developing a Nowcasting Capability for X lass Solar Flares Using VLF Radiowave Propagation Changes Space Weather, 2019, 17, 1783-1799.	3.7	12
177	Calculation of GIC in the North Island of New Zealand Using MT Data and Thinâ€Sheet Modeling. Space Weather, 2020, 18, e2020SW002580.	3.7	12
178	Testing the formulation of Park and Dejnakarintra to calculate thunderstorm dc electric fields. Journal of Geophysical Research, 1998, 103, 2171-2178.	3.3	11
179	A statistical approach to determining energetic outer radiation belt electron precipitation fluxes. Journal of Geophysical Research: Space Physics, 2014, 119, 3961-3978.	2.4	11
180	Semi-annual oscillation (SAO) of the nighttime ionospheric DÂregion as detected through ground-based VLF receivers. Atmospheric Chemistry and Physics, 2016, 16, 3279-3288.	4.9	11

#	Article	IF	CITATIONS
181	Geomagnetically induced currents during the 07–08 September 2017 disturbed period: a global perspective. Journal of Space Weather and Space Climate, 2021, 11, 33.	3.3	11
182	The Impact of Sudden Commencements on Ground Magnetic Field Variability: Immediate and Delayed Consequences. Space Weather, 2021, 19, e2021SW002764.	3.7	11
183	Geomagnetically Induced Current Model in New Zealand Across Multiple Disturbances: Validation and Extension to Nonâ€Monitored Transformers. Space Weather, 2022, 20, .	3.7	11
184	Dregion reflection height modification by whistler-induced electron precipitation. Journal of Geophysical Research, 2002, 107, SIA 18-1.	3.3	10
185	A Multiâ€Instrument Approach to Determining the Sourceâ€Region Extent of EEPâ€Driving EMIC Waves. Geophysical Research Letters, 2020, 47, e2019GL086599.	4.0	10
186	Energetic electron precipitation characteristics observed from Antarctica during a flux dropout event. Journal of Geophysical Research: Space Physics, 2013, 118, 6921-6935.	2.4	9
187	Observations of nitric oxide in the Antarctic middle atmosphere during recurrent geomagnetic storms. Journal of Geophysical Research: Space Physics, 2013, 118, 7874-7885.	2.4	9
188	The world wide lightning location network (WWLLN): Update of status and applications. , 2014, , .		9
189	Techniques to determine the quiet day curve for a long period of subionospheric VLF observations. Radio Science, 2015, 50, 453-468.	1.6	9
190	Solar proton events and stratospheric ozone depletion over northern Finland. Journal of Atmospheric and Solar-Terrestrial Physics, 2018, 177, 218-227.	1.6	9
191	Magnetic Local Timeâ€Resolved Examination of Radiation Belt Dynamics during Highâ€Speed Solar Wind Speedâ€Triggered Substorm Clusters. Geophysical Research Letters, 2019, 46, 10219-10229.	4.0	9
192	Electron Precipitation From the Outer Radiation Belt During the St. Patrick's Day Storm 2015: Observations, Modeling, and Validation. Journal of Geophysical Research: Space Physics, 2020, 125, e2019JA027725.	2.4	9
193	Linkages Between the Radiation Belts, Polar Atmosphere and Climate: Electron Precipitation Through Wave Particle Interactions. , 2016, , 354-376.		9
194	Investigating radiation belt losses though numerical modelling of precipitating fluxes. Annales Geophysicae, 2004, 22, 3657-3667.	1.6	9
195	A vertical-plasma-slab model for determining the lower limit to plasma density in sprite columns from VLF scatter measurements. IEEE Antennas and Propagation Magazine, 1997, 39, 44-53.	1.4	8
196	Investigating the possible association between thunderclouds and plasmaspheric ducts. Journal of Geophysical Research, 2001, 106, 29771-29781.	3.3	8
197	A quantitative examination of lightning as a predictor of peak winds in tropical cyclones. Journal of Geophysical Research D: Atmospheres, 2015, 120, 3789-3801.	3.3	8
198	Long-term climate change in the D-region. Scientific Reports, 2017, 7, 16683.	3.3	8

#	Article	IF	CITATIONS
199	Dâ€Region High‣atitude Forcing Factors. Journal of Geophysical Research: Space Physics, 2019, 124, 765-781.	2.4	7
200	The Source Regions of Whistlers. Journal of Geophysical Research: Space Physics, 2019, 124, 5082-5096.	2.4	7
201	Examination of Radiation Belt Dynamics During Substorm Clusters: Activity Drivers and Dependencies of Trapped Flux Enhancements. Journal of Geophysical Research: Space Physics, 2022, 127, .	2.4	7
202	Identifying power line harmonic radiation from an electrical network. Annales Geophysicae, 2005, 23, 2107-2116.	1.6	6
203	Comment on "Preseismic Lithosphere-Atmosphere-Ionosphere Coupling― Eos, 2007, 88, 248-248.	0.1	6
204	Quiet Daytime Arctic IonosphericDRegion. Journal of Geophysical Research: Space Physics, 2018, 123, 9726-9742.	2.4	6
205	Predicting Lower Band Chorus With Autoregressiveâ€Moving Average Transfer Function (ARMAX) Models. Journal of Geophysical Research: Space Physics, 2019, 124, 5692-5708.	2.4	6
206	Solar flare Xâ€ r ay impacts on long subionospheric VLF paths. Space Weather, 2021, 19, e2021SW002820.	3.7	6
207	Radiating conducting columns inside the Earth–ionosphere waveguide: Application to red sprites. Journal of Atmospheric and Solar-Terrestrial Physics, 1998, 60, 1177-1204.	1.6	5
208	Position determination of red sprites by scattering of VLF subionospheric transmissions. Geophysical Research Letters, 1998, 25, 281-284.	4.0	5
209	Lightning atmospherics count rates observed at Halley, Antarctica. Journal of Atmospheric and Solar-Terrestrial Physics, 2001, 63, 993-1003.	1.6	5
210	High-latitude geomagnetically induced current events observed on very low frequency radio wave receiver systems. Radio Science, 2010, 45, n/a-n/a.	1.6	5
211	Tropical daytime lower Dâ€region dependence on sunspot number. Journal of Geophysical Research, 2012, 117, .	3.3	5
212	Investigating the upper and lower energy cutoffs of EMIC-wave driven precipitation events. , 2014, , .		5
213	Investigating Dunedin whistlers using volcanic lightning. Geophysical Research Letters, 2014, 41, 4420-4426.	4.0	5
214	Groundâ€Based Observations of VLF Waves as a Proxy for Satellite Observations: Development of Models Including the Influence of Solar Illumination and Geomagnetic Disturbance Levels. Journal of Geophysical Research: Space Physics, 2019, 124, 2682-2696.	2.4	5
215	Evidence of Subâ€MeV EMICâ€Driven Trapped Electron Flux Dropouts From GPS Observations. Geophysical Research Letters, 2021, 48, e2021GL092664.	4.0	5
216	Cross―Coherence of the Outer Radiation Belt During Storms and the Role of the Plasmapause. Journal of Geophysical Research: Space Physics, 2021, 126, e2021JA029308.	2.4	5

#	Article	IF	CITATIONS
217	Correction to "Are whistler ducts created by thunderstorm electrostatic fields?―by C. J. Rodger et al Journal of Geophysical Research, 2002, 107, SIA 1-1.	3.3	4
218	What Fraction of the Outer Radiation Belt Relativistic Electron Flux at L â‰^ 3â€4.5 Was Lost to the Atmosphere During the Dropout Event of the St. Patrick's Day Storm of 2015?. Journal of Geophysical Research: Space Physics, 2019, 124, 9537-9551.	2.4	4
219	Comparison of Multiple and Logistic Regression Analyses of Relativistic Electron Flux Enhancement at Geosynchronous Orbit Following Storms. Journal of Geophysical Research: Space Physics, 2019, 124, 10246-10256.	2.4	4
220	Impact of EMICâ€Wave Driven Electron Precipitation on the Radiation Belts and the Atmosphere. Journal of Geophysical Research: Space Physics, 2021, 126, e2020JA028671.	2.4	4
221	Quiet Night Arctic Ionospheric <i>D</i> Region Characteristics. Journal of Geophysical Research: Space Physics, 2021, 126, e2020JA029043.	2.4	4
222	Outer Van Allen belt trapped and precipitating electron flux responses to two interplanetary magnetic clouds of opposite polarity. Annales Geophysicae, 2020, 38, 931-951.	1.6	4
223	The impact of PMSE and NLC particles on VLF propagation. Annales Geophysicae, 2004, 22, 1563-1574.	1.6	3
224	Spatial Distributions of Nitric Oxide in the Antarctic Wintertime Middle Atmosphere During Geomagnetic Storms. Journal of Geophysical Research: Space Physics, 2020, 125, e2020JA027846.	2.4	3
225	Comparison of Longâ€Term Lightning Activity and Inner Radiation Belt Electron Flux Perturbations. Journal of Geophysical Research: Space Physics, 2020, 125, e2019JA027763.	2.4	3
226	Impacts of UV Irradiance and Medium-Energy Electron Precipitation on the North Atlantic Oscillation during the 11-Year Solar Cycle. Atmosphere, 2021, 12, 1029.	2.3	3
227	The Correspondence Between Sudden Commencements and Geomagnetically Induced Currents: Insights From New Zealand. Space Weather, 2022, 20, .	3.7	3
228	Daytime VLF modeling over land and sea, comparison with data from DEMETER satellite. , 2011, , .		2
229	PLASMON: Data assimilation of the Earth's plasmasphere. , 2011, , .		2
230	Remote sensing space weather events through ionospheric radio: The AARDDVARK network. , 2014, , .		2
231	Very low frequency radio events with a reduced intensity observed by the lowâ€altitude DEMETER spacecraft. Journal of Geophysical Research: Space Physics, 2015, 120, 9781-9794.	2.4	2
232	Observed response of stratospheric and mesospheric composition to sudden stratospheric warmings. Journal of Atmospheric and Solar-Terrestrial Physics, 2019, 191, 105054.	1.6	2
233	VLF scattering from red sprites: vertical columns of ionisation in the Earth-ionosphere waveguide. , 0, , .		1
234	Correction to "Radiation belt electron precipitation by man-made VLF transmissions― Journal of Geophysical Research, 2009, 114, n/a-n/a.	3.3	1

#	Article	IF	CITATIONS
235	Correction to "Radiation belt electron precipitation into the atmosphere: Recovery from a geomagnetic storm― Journal of Geophysical Research, 2010, 115, .	3.3	1
236	Automatic retrieval of plasmaspheric electron densities: First results form Automatic Whistler Detector and Analyzer Network. , 2011, , .		1
237	Detecting space weather events with subionospheric VLF observations: Producing quiet day curves from AARDDVARK data. , 2014, , .		1
238	Testing AIMOS ionization rates in the middle atmosphere: Comparison with ground based radio wave observations of the ionosphere. , 2014, , .		1
239	Ground-based very-low-frequency radio wave observations of energetic particle precipitation. , 2020, , 257-277.		1
240	Satellite and ground-based observations of a large-scale electron precipitation event. , 2011, , .		0
241	Relativistic microburst storm characteristics: Combined satellite and ground-based observations. , 2011, , .		0
242	Remote sensing space weather events through ionospheric radio: The AARDDVARK network. , 2011, , .		0
243	Statistical analysis of outer electron radiation belt dropouts: geosynchronous and low earth orbit responses during solar wind stream interfaces. , 2011, , .		0
244	Unusual observation of chorus at L=2.6. , 2011, , .		0
245	Investigating electron precipitation event characteristics and drivers: Combining BARREL-inspired measurements from Antarctica and Canada. , 2014, , .		Ο
246	Calibration of electron density obtained from whistler inversion with in-situ satellite measurements. , 2014, , .		0
247	The role of the plasmapause on energetic electron precipitation fluxes during space weather events. , 2014, , .		0
248	Remote sensing space weather events through ionospheric radio: Latest update from the AARDDVARK network. , 2014, , .		0
249	Long term determination of variations in energetic electron precipitation into the atmosphere using AARDDVARK. , 2014, , .		0
250	Embodied Earth: Experiencing natural phenomena. , 2016, , .		0
251	Very Low Latitude Whistlerâ€Mode Signals: Observations at Three Widely Spaced Latitudes. Journal of Geophysical Research: Space Physics, 2019, 124, 9253-9269.	2.4	0
252	4.5 Atmospheric ionisation by solar energetic particle precipitation. , 2015, , .		0